Mat. Res. Soc. Symp. Proc. Vol. 784 © 2004 Materials Research Society C5.8

Microwave Properties of Parallel Plate Capacitors based on $(Ba,Sr)TiO_3$ Thin Films Grown on SiO_2/Al_2O_3 Substrates

I.P. Koutsaroff, T. Bernacki, M. Zelner, A. Cervin-Lawry, A. Kassam, P. Woo, L. Woodward, and A. Patel
Gennum Corporation, 970 Fraser Drive, Burlington, Ontario L7L 5P5 Canada
ikoutsar@gennum.com

ABSTRACT

$Ba_{0.7}Sr_{0.3}TiO_3$ (BST) single and quadruple layer capacitors with Pt electrodes were fabricated together on polycrystalline alumina substrates with a SiO_2-based multicomponent amorphous buffer layer (SiO_2/Al_2O_3). This paper presents the results of the characterization of these capacitors, to demonstrate their suitability for application as decoupling (high value) capacitors and as components in tunable RF applications (e.g., phase shifters and filters). BST films of different compositions, $(Ba_{0.7}Sr_{0.3})TiO_3$ and $(Ba_{0.5}Sr_{0.5})TiO_3$, were grown by metal-organic decomposition (MOD) and RF magnetron reactive sputtering. The capacitance density of 90-140 nm thick BST films was in the range of 20 to 70 fF/μm^2. Parallel plate capacitors with areas from 16 μm^2 to 2.25 mm^2 were fabricated using photolithography and ion milling techniques. For large capacitors (0.125 to 2.25 mm^2), capacitance and tanδ were measured at low frequencies (1 KHz - 1 MHz) using an LCR meter. Smaller capacitors (16 μm^2 to 3600 μm^2) were additionally characterized in the frequency range of 50 MHz - 20 GHz. In such case, capacitance, tanδ and equivalent series resistance (ESR) were extracted from two port scattering parameters obtained using a vector network analyzer (VNA). The relationship between dielectric loss, tunability and calculated figure of merit vs. BST composition and deposition temperature was outlined. In addition, loss and ESR at high frequencies was investigated. The typical achieved leakage current density of sputtered BST films for 2.25 mm^2 capacitors fabricated on SiO_2/Al_2O_3 was 7.3×10^{-9} A/cm^2 at 300 kV/cm (65 fF/μm^2), about 2 times lower than for $(Ba_{0.7}Sr_{0.3})TiO_3$ films deposited by MOD (1.4×10^{-8} A/cm^2 at 300 kV/cm, 34.5 fF/μm^2). Furthermore, the tunability of $(Ba_{0.7}Sr_{0.3})TiO_3$ deposited by both methods on SiO_2/Al_2O_3 was ~60% at 350 kV/cm.

INTRODUCTION

Barium Strontium Titanate (BST) is an important material used in integrated passive devices, decoupling capacitors [1], multi-chip modules (MCM), and chip-scale packaging. BST also has shown great potential for the fabrication of tunable RF devices [2, 3] such as voltage-controlled oscillators [4], tunable filters [5], and phase shifters [6]. BST forms a solid solution for all Ba/Sr ratios that makes it ideally suitable for the wide temperature range of applications. Based on the required thickness and microstructure, BST thin films might be deposited by a variety of deposition techniques, such as MOCVD [7], CSD(MOD) [8], RF magnetron reactive sputtering [9, 10], etc. However, the combination of critical properties such as high dielectric constant, low loss, low leakage current and high tunability have not been achieved simultaneously. The ability to reproducibly grow BST films on commercially available large size substrates, which have both low loss and high tunability is a critical requirement for large volume manufacturing of tunable microwave components. However different combinations of parameters are critical for decoupling applications, namely high capacitance and low leakage current. Thin film BST-based decoupling capacitors can be fabricated with high yield, reproducibility and high capacitance

density (e.g., from 30 to 53 $fF/\mu m^2$ per single layer and from 120 to 300 $fF/\mu m^2$ for multiple layers) on Si substrates [10, 11, 12]. Extensive studies of BST films deposited on $LaAlO_3$ (100), MgO (100) and other single crystal substrates indicate that there is a dependence of the capacitance and dissipation factors of these films on the substrate type [3, 13].

The permittivity of BST films is dependent on the film composition and can be tuned by an applied DC electric field. In parallel plate capacitors, tunability as high as 53% has been achieved at DC bias voltages as low as 3.2 V(200kV/cm) with a capacitance density of 48 $fF/\mu m^2$ for a BST film deposited by PLD on SiO_2/Si [14]. So far the highest tunability of 75% was achieved for epitaxial BST films on $LaAlO_3$ at 750 ^oC by PLD, with a thickness of 0.5 μm at a DC bias voltage of 3.4 V [15]. The effect of lattice distortions (e.g., microstrains ($\Delta a/a$)) and the film stress, due to the thermal expansion mismatches between the film and substrate, have a crucial impact on DC tunability [16], BST dielectric losses and microwave quality factor [17]. The last study showed that the most appropriate combination from the point of view of RF and microwave devices, including low dielectric loss, high tunability and minimum deviation of the temperature of maximum $\varepsilon(T)$, is observed only for BST/α-Al_2O_3 structures. In this context, it is also our view that polycrystalline Al_2O_3 is the most suitable substrate for RF applications because of its stability at high temperatures and low loss at high frequencies (5-20 GHz) [18]. It is well known that different deposition techniques for BST films show different residual stress, microstructure, grain size and orientation. So far, no complete data have been reported for BST films grown by different methods for further optimization of BST film properties for integrating decoupling capacitors and tunable RF components on the same Al_2O_3 substrate.

In the present study, we fabricated stoichiometric BST films of 2 different compositions by CSD method as well as by high temperature RF magnetron sputtering on SiO_2/Al_2O_3 substrates.

EXPERIMENTAL PROCEDURE

Two types of 4” substrates were used in the current studies: polycrystalline alumina substrates with a SiO_2-based multicomponent amorphous buffer layer (SiO_2/Al_2O_3), and Si control wafers (thermally oxidized low resistivity, n-type Silicon <111>). Both types of substrates have a TiO_x adhesion layer and DC sputtered 150-200 nm Pt electrodes. The BST film composition was Ba:Sr:Ti = 0.7:0.3:1.0 and Ba:Sr:Ti = 0.5:0.5:1.0. Details on CSD(MOD) conditions and formation of parallel plate multilayer capacitors have been given elsewhere [11, 19]. For the RF-magnetron sputtering experiments the following conditions were used: target composition, Ba:Sr=0.5:0.5 or Ba:Sr=0.7:0.3, Ar:O_2 ratio of 6:1, sputtering pressure of 15 mTorr, RF power density of 2.0 W/cm^2 and deposition rate of 6 nm/min. Further details have been provided in ref. [9] and [20]. After formation of the BST films by both deposition techniques the samples were deposited with 200nm top Pt electrodes. Ar ion milling was used to pattern the multilayer Pt/BST/Pt stack. The structure was subsequently annealed in O_2 at a similar temperature to the initial BST film processing temperature (600-800 ^oC).

RESULTS AND DISCUSSION

Film Morphology

An investigation of the surface morphology of the BST films was carried out by FE-SEM. Figure 1 shows FE-SEM microphotographs of RF sputtered BST films deposited on $Pt/TiO_x/SiO_2/Si$ substrates for both compositions: $(Ba_{0.5}Sr_{0.5})TiO_3$ and $(Ba_{0.7}Sr_{0.3})TiO_3$. Films were processed at 600 °C and 750 °C respectively. The BST films grown at a higher temperature and with a higher

Ba content show similar sizes of crystallites populating the surface.

The main difference in the BST films is the smaller surface roughness in the case of the BST sputtered film at lower temperature. The degree of film densification and the size of specific defects (i.e., pores, grain boundaries, cavities, etc.) is strongly dependent on the processing temperature and substrate type. BST films sputtered at 750 °C on SiO_2/Si show more densely packed fine grains with a more pronounced columnar structure compared to BST films processed at 600 °C. The higher degree of columnar crystal habit of $(Ba_{0.7}Sr_{0.3})TiO_3$ films could be also responsible for better dielectric properties in addition to the well known effect of increased grain size with processing temperature as observed in previous studies [21]. Surface morphology of CSD deposited BST films on Al_2O_3 substrates were reported previously [19].

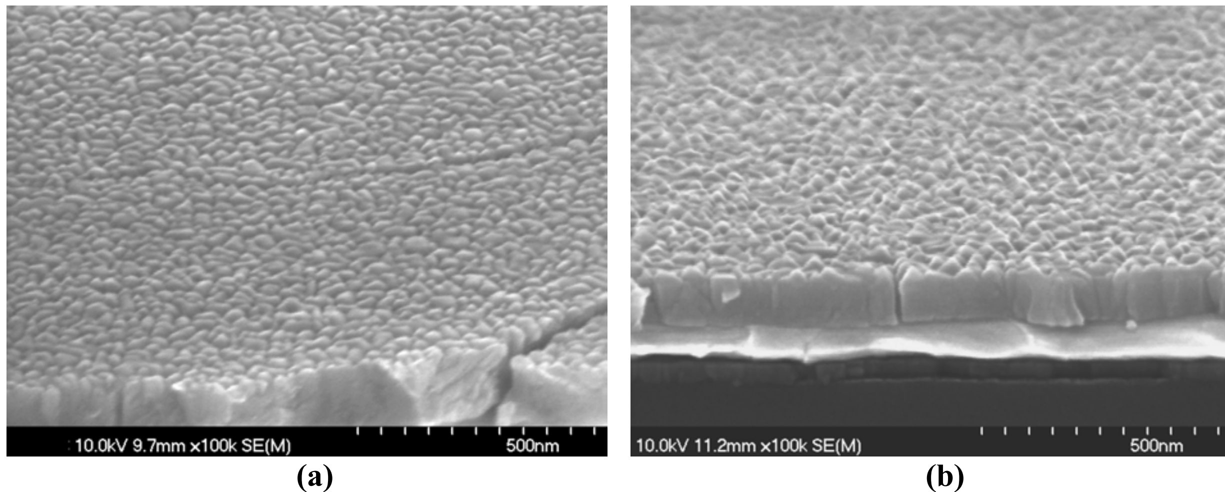

Fig. 1. FE-SEM of (a) 0.12 μm thick $(Ba_{0.5}Sr_{0.5})TiO_3$ films and (b) 0.1 μm thick $(Ba_{0.7}Sr_{0.3})TiO_3$, both on on Pt/TiO_x/SiO_2/Si.

The effects of substrate temperature during RF sputtering on the degree of BST crystallinity were also studied. Films grown on SiO_2/Si(111) were compared structurally. From all BST XRD peaks, the most intense was (110) with 2θ value at 31.75°, while the (111) peak at 39.2° is overlapped with the Pt(111) peak. It is seen that (110) reflection has higher intensity for BST grown at higher temperatures [20]. Based on the analysis of experimental data, all samples (including the CSD ones [19]) show almost identical diffraction patterns and are attributed to cubic (perovskite) crystal symmetry.

Electrical Characteristics

Electrical characterization was carried out using a HP4284A LCR meter from frequencies of 100 Hz to 1 MHz. C-V properties were established, and low frequency capacitance and loss were obtained from 30-100 devices over 2-3 wafers for each processing condition. Current-voltage characteristics were obtained using a Keithley 236 Source-Measure unit. Characterization from 100 MHz to 20 GHz was performed using a HP8720C Vector Network Analyzer and Cascade probes. All measurements were performed at wafer level.

Tunability, leakage current, and high frequency characteristics were only obtained after the completion of the metal interconnect. Capacitors 1500, 60, 20, 18, 15 and 4 μm on a side were measured. The designed device size varied from sample to sample.

Table I: Sample deposition conditions summary

Sample	BST Film Thicknes (nm)	Proces. Temp. (oC)	Deposition method	Ba Comp.	Substrate
S1	90	700	RF sputter	x=0.7	SiO_2/Al_2O_3
S2	140	670	CSD	x=0.7	SiO_2/Al_2O_3
S3	120	600	RF sputter	x=0.5	SiO_2/Al_2O_3
S4	140	800	CSD	x=0.7	SiO_2/Si
S5	140	670	CSD	x=0.7	SiO_2/Al_2O_3
S6	100	625	RF sputter	x=0.7	SiO_2/Al_2O_3

Table I and Table II (a) and (b) summarize the sample history and results for the samples. Table II(a) shows results for the largest capacitors (1500x1500 µm). Table II(b) shows the results for capacitors of size 5-20 µm per side (depending on the sample), focusing on parameters critical to performance in high-frequency applications such as tunability (defined as $(C_o-C_v)/C_o$) and figure of merit (FOM, defined as tunability/tanδ) [3].

Table II: Capacitors characteristics sample summary

Capacitor characteristics for 1500x1500 µm decoupling capacitors (a), and capacitor characteristics for small (15x15, 18x18 and 20x20) high frequency capacitors (b), integrated on the same substrates. Measurements performed at 10 kHz.

Sample	Capacitance Density (fF/um^2)	tanδ	Current Density @ 200 kV (A/cm^2)	Current Density @ 300 kV (A/cm^2)
S1	65.5	0.026	7.22×10^{-9}	9.25×10^{-9}
S2	34.4	0.019	3.96×10^{-9}	2.35×10^{-8}
S3	20.3	0.0117	2.74×10^{-9}	2.58×10^{-9}
S4	28.8	0.012	5.20×10^{-9}	9.74×10^{-8}
S5	33.7 *	0.026	5.09×10^{-9}*	7.33×10^{-8}*

(a)

Sample	tanδ	Tunability @ 350 kV	FOM
S1	0.0127	60%	47.2
S2	0.0079	58%	73.0
S3	0.0062	37%	59.0
S6	0.0086	54%	62.7

(b)

* Normalized effective capacitance density per layer (134.8 $fF/\mu m^2$ in total) and leakage current density per layer averaged from 4 layers connected in parallel.

Low frequency (10 KHz with 0.1 V signal level) electrical measurements of capacitance of $(Ba_{0.7}Sr_{0.3})TiO_3$ and $(Ba_{0.5}Sr_{0.5})TiO_3$ planar capacitors (250x500 μm^2) deposited at a temperature range of 600°C to 800°C by CSD and RF sputtering on 2 different types of substrates are shown in Fig. 1.

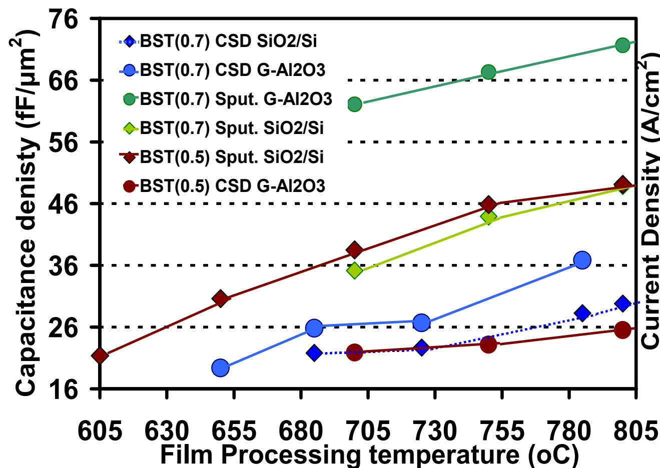

Fig. 1. Capacitance of BST (x=0.7 and x=0.5) capacitors on 2 different substrates, deposited by CSD and RF sputtering at different temperatures.

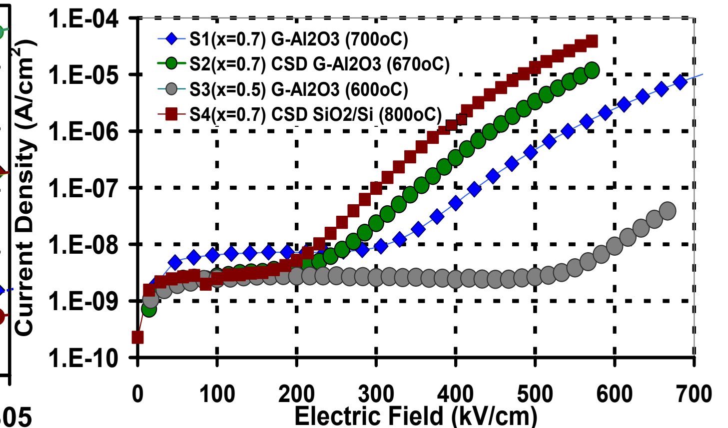

Fig. 2. Leakage current density versus electric field for BST (x=0.7 and x=0.5) capacitors on 2 different substrates, deposited by CSD and RF sputtering (1 sec settling and delay time, 0.2 V step).

The leakage current of several samples is shown in Fig. 2. It can be seen that despite the increased capacitance density of sample S1 (concurrent with an increased loss tangent), leakage is only twice the CSD control (S2) below 3V, but is similar to S3 and better than S2, S4, and S5 for greater than 3V, with the exception of sample S3, which displays an unusually wide flat Ohmic current region with a transition electric field of 530 kV/cm (6.4V).

Tunability of the samples is shown in Fig.3 (a) and Fig.3 (b). Figure 3(a) shows the tunability versus electric field. It can be seen that the tunability of the film depends only on the BST film composition and substrate material, and not on deposition temperature (from 650 oC to 800 oC, $(Ba_{0.7}Sr_{0.3})TiO_3$). This behaviour is contrary to that reported in the literature, e.g., PLD grown BST on MgO (650-875°C) [22]. The exact reasons for this have yet to be explored. When the tunability versus applied voltage is examined, however, sample S1, having a thinner dielectric, is found to have exceptionally high tunability, achieving 60% at an applied voltage of only 3V (350 kV/cm). This is very close or better than the best reported in the literature for RF sputtered or PLD deposited films (53% at 4V(500kV/cm), 80nm [23]; 58% at 2.4V(80kV/cm), 300nm [22]).

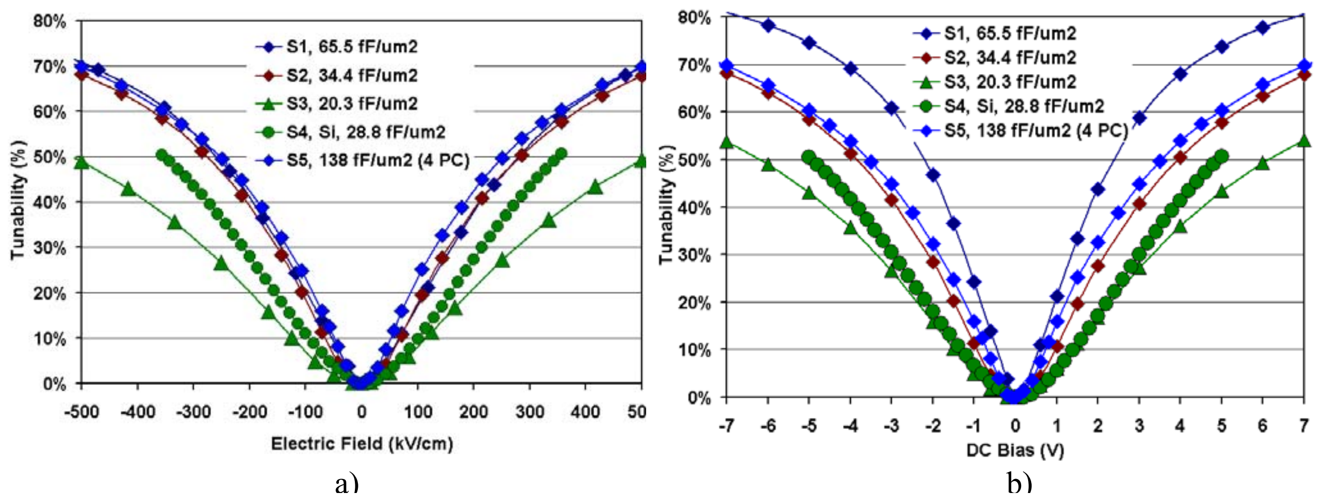

Fig. 3. Tunability of BST capacitors as a function of applied electric field and voltage bias.

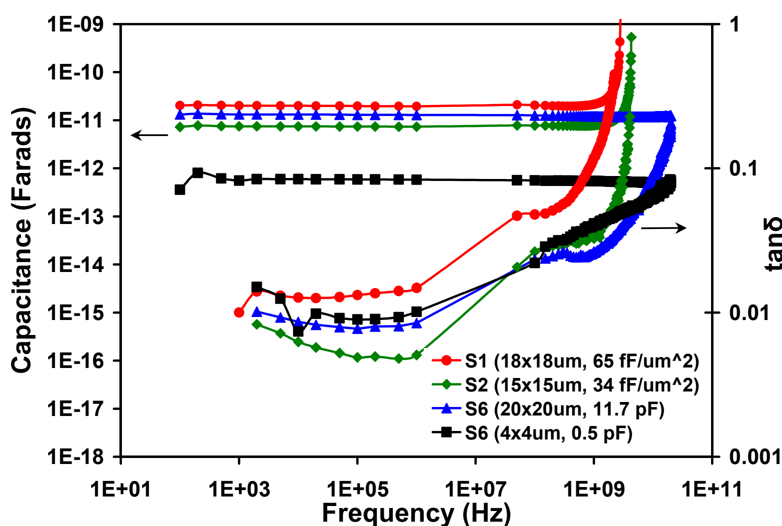

Fig. 4 Capacitance vs. frequency for small BST parallel plate capacitors on SiO_2/Al_2O_3 with different dielectric properties.

The deposited BST films show good high frequency performance. Fig. 4 shows the behaviour of small capacitors versus frequency. Sample S6 utilized more advanced techniques to remove test fixture parasitics [24] and does not show the series self-resonance that is observed in the capacitors from samples S1 and S2, displaying flat capacitance behaviour to 20 GHz. Coincident with the sharp increase in observed capacitance due to self-resonance, a rapid increase in tanδ is also observed

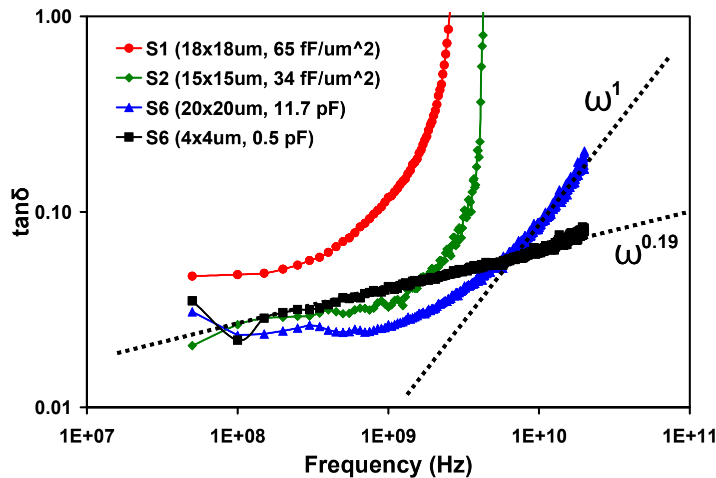

Fig. 5 Frequency dependence of dielectric loss tangent.

in samples S1 and S2. The capacitors of sample S6 do not display a self-resonance, but nevertheless shows a frequency dependence. If the loss in the device is assumed to be due to a series combination of electrode resistance and a frequency-independent dielectric loss alone, then the calculated device loss tangent is equal to $\tan\delta_{mat}+R_e\omega C$, where R_e is the electrode resistance and $\tan\delta_{mat}$ is the actual BST material loss tangent. It can be seen that the total device loss tangent will closely approximate the material loss tangent at low frequencies, but will increase linearly at higher frequencies due to the non-zero electrode resistance. This is observed in sample S6 (20x20 μm, 11.7 pF), where tanδ increases proportionally to ω at high frequencies. The smaller capacitor S6 (4x4 μm, 0.5 pF) does not display the linear increase due to much lower electrode resistance and capacitance. However, a frequency dependence proportional to approximately $\omega^{0.19}$ is observed (see Fig. 5). Dielectric loss behaviour similar to this has been observed by other research groups, with the exact dependence ranging from $\omega^{0.1}$ [25] to $\omega^{0.33}$ [26]. A frequency dependent AC leakage component at so-called intermediate frequencies (above the region where DC leakage dominates loss and below where electrode losses dominate) has been proposed to model the observed losses [25]. The behaviour has been attributed to relaxation losses (Debye mechanism) due to the field generated by charged defects, with the exact frequency dependence determined by the size distribution of the charged regions [26-28].

CONCLUSIONS

We observed higher BST capacitance density (65-70 fF/μm^2) on alumina-based substrates compared to control SiO_2/Si substrates (28-49 fF/μm^2) when grown at the same conditions. The higher capacitance per unit area on alumina was usually accompanied with lower or similar leakage current densities in the thermionic emission region.

The present studies of the tunability of BST films at various processing conditions showed primary dependence on film composition, and no significant effect from thickness, processing temperatures (650-800 ^{o}C), or deposition method. Further studies may identify the exact mechanisms that contribute to dissipation factor and tunability characteristics.

The feasibility of using the same deposited BST film for both decoupling and high frequency tunable applications has been demonstrated, in both single layer and multiple layer architectures. This work opens an avenue for optimization of individual layers in multilayer structures for either decoupling or high frequency applications, integrated on the same substrate.

ACKNOWLEDGEMENTS

The authors would like to acknowledge the contributions of Dr. K. Suu, Dr. T. Jimbo (Ulvac, Inc.) for RF sputtered BST sample preparation and useful discussions, as well as our appreciation to Carol Wood and Shirley Lavigne for the experimental work supporting this paper.

REFERENCES

[1] M. Watt, WO9800871, (1998).
[2] A. Tombak, J.-P. Maria, F. Ayguavives, Z. Jin, G.T. Stauf, A.I. Kingon, IEEE Microwave and Wireless Components Letters, **12**, 3 (2002).
[3] X.H. Zhu, J.M. Zhu, S.H. Zhou, Z.G. Liu, N.B. Ming, S.G. Lu, H.L.W.Chan, C.L. Choy, Journal of Electronic Materials, **32**, 1125 (2003).
[4] O.G. Vendik, Ferroelectrics **12**, 85 (1976).
[5] A. Tombak, J.-P. Maria, F.T. Ayguavives , Z. Jin, G.T. Stauf, A.I. Kingon, A. Mortazawi IEEE Trans. on Microwave Theory and Techniques, **51**, 462 (2003).
[6] B. Acikel B, T.R. Taylor, P.J. Hansen, J.S. Speck, R.A York, IEEE Microwave and Wireless Components Letters, **12**, 237 (2002).
[7] C. B. Parker, J.-P. Maria, A. I. Kingon, Appl. Phys. Lett., **81**, 340 (2002).
[8] S. Halder, T. Schneller, R. Waser, Mat. Res. Soc. Symp. Proc., Vol. 762, C8.17.1 (2003).
[9] B. A. Baumert, L.-H. Chang, A. T. Matsuda, T.-L. Tsai, C. J. Tracy, R. B. Gregory, P. L. Fejes, N. G. Cave, W. Chen, D. J. Taylor, T. Otsuki, E. Fujii, S. Hayashi, K. Suu, J. Appl. Phys., **82**, 2558 (1997).
[10] J.D.Baniecki, T. Shiroga and K. Kurihara, Integrated Ferroelectrics, **46**, 221 (2002).
[11] Watt, M.M., P. Woo, T. Rywak, L. McNeil, A. Kassam, ISAF 98, Proc. of the 11th IEEE Inter. Symp. on Applications of Ferroelectrics, 11, (1998).
[12] Y. Takeshima, K. Tanaka, Y. Sakabe, Ceramic Transactions, **106**, 441 (2000).
[13] S. Horwitz, W.T. Chang, W. Kim, S.B. Qadri, J.M. Pond, S.W. Kirchoefer, D.B. Chrisey, J. of Electroceramics, **4**, 357, (2000).
[14] Young-Ah Jeon, W-C. Shin, T-S. Seo, S-G. Yoon, J. Mater. Res., **17**, 2831, (2002).
[15] W. Chang, C. M. Gilmore, W.-J. Kim, J. M. Pond, S. W. Kirchoefer, S. B. Qadri, D. B. Chrisey, and J. S. Horwitz, J. Appl. Phys. **87**, 3044 (2000).
[16] W. Chang, S.W. Kirchoefer, J.M. Pond, and J.S. Horwitz, L. Sengupta, J. of Appl. Phys., **92**, 1528 (2002).
[17] S.F. Karmanenko, A.I. Dedyk, A.A. Melkov, R. N. Il'in, V.I. Sakharov, I.T. Serenkov and J. Ha, J. Phys.: Condens. Matter, **14**, 6823 (2002).
[18] A. Cervin-Lawry A, K. Ali, T. Bernacki, S. Binapal, C. Miortescu, A. Patel, P. Woo, L. Woodward, Proc. of SPIE, Vol. 5231, 7, (2003).
[19] I.P. Koutsaroff, A. Kassam, M. Zelner, P. Woo, L. McNeil, T. Bernacki, A. Cervin-Lawry, and A. Patel, Mat. Res. Soc. Symp. Proc. Vol. 748, U6.1.1 (2002).
[20] T. Jimbo, I. Kimura, Y. Nishioka, K. Suu, Mat. Res. Soc. Symp. Proc. Vol. 762, C7.8.1 (2003) (in press).
[21] T. Horikawa, N. Mikami, H. Ito, Y. Ohno, T. Makita, K. Sato, IEICE Trans. Electron., Vol. E77-C, 385 (1994).
[22] B.H. Park, Q. Jia, Jpn. J. Appl. Phys., 1 **41**, 7222 (2002).
[23] J. Im, O. Auciello, P. K. Baumann, and S. K. Streiffer, D.Y. Kaufman, A.R. Krauss, Appl. Phys. Lett., **76**, 625 (2002).
[24] K. Ikuta, Y. Umeda, Y. Ishii, Jpn. J. Appl. Phys. 2 **34**, L1211 (1995).
[25] B. York, "Thin-Film BST for Tunable Integrated Passives", IMS 2003 Ferroelectric Workshop, June 2003.
[26] O. G. Vendik, A. N. Rogachev, Tech. Phys. Lett., **25**, 702 (1999).
[27] O. G. Vendik, L. T. Ter-Martirosyan, S. P. Zubko, J. Appl. Phys., **84**, 993 (1998).
[28] M. Furuya, J. Appl. Phys., **85**, 1084 (1999).